

# A hydraulic driver system for MR elastography of small animals

M. Neumaier<sup>1</sup>, E. Schuck<sup>2</sup>, T. Kaulisch<sup>1</sup>, H. G. Niessen<sup>1</sup>, D. Klatt<sup>3</sup>, I. Sack<sup>3</sup>, J. Braun<sup>4</sup>, and D. Stiller<sup>1</sup>

<sup>1</sup>In-Vivo Imaging Unit, Dept. of Drug Discovery Support, Boehringer Ingelheim Pharma GmbH & Co. KG, Biberach, BW, Germany, <sup>2</sup>Precision Mechanics, Dept. of Site Operations, Boehringer Ingelheim Pharma GmbH & Co. KG, Biberach, BW, Germany, <sup>3</sup>Dept. of Radiology, Charité - University Medicine Berlin, Berlin, Germany, <sup>4</sup>Dept. of Medical Informatics, Charité - University Medicine Berlin, Berlin, Germany

## Introduction:

MR elastography [1] is a non-invasive imaging technique capable to assess the stage of non-alcoholic fatty liver diseases with high sensitivity and specificity in animal models [2] as well as in man [3]. The method relies on the measurement and analysis of shear waves in the acoustic frequency range between 25 and 1000 Hz. For generating vibrations in MRE a variety of driver systems has been proposed particularly dedicated to phantom studies or in-vivo experiments on clinical human MRI scanners [4]. Only few MRE driver systems have been described in literature, which are applicable to small animal MRI systems. Two challenges arise in MRE on small animal systems: i) limited space for in situ wave generation and ii) small fields of view requiring high vibration frequencies in order to reduce wavelengths. The standard approach in this type of MRE experiments is the use of elongated rigid transducers connecting a vibration generator with the surface of the animal. This approach is limited in flexibility of source positioning and animal handling. Therefore, a new hydraulic transducer driven by a piezoelectric vibrator was developed. This kind of system enables a mechanical excitation in small animal scanners, offers flexible positioning of actuators with little interaction with magnetic fields and insignificant image distortions. The objective of this study was to test the applicability of the hydraulic based actuator for MRE of small animals with high frequency mechanical excitation.

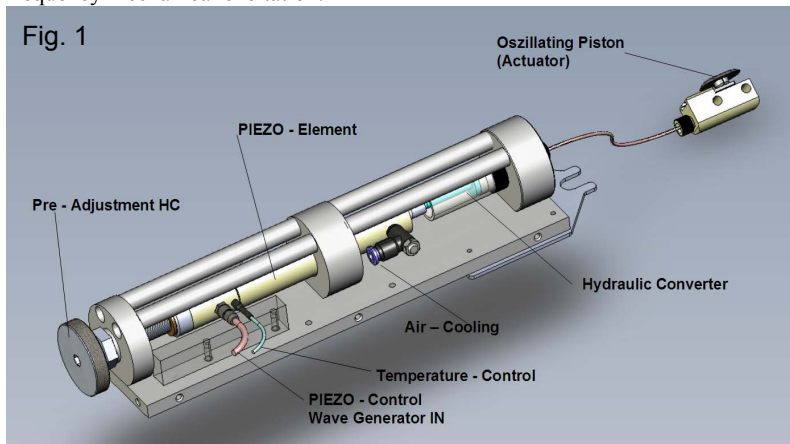


**Fig.1:** Sketch of the proposed hydraulic drive system of a piezoelectric element driving a hydraulic converter connected via a highly rigid hydraulic tube to an oscillating piston at the end of the line. The maximum elongation of the piezoelectric element is 150  $\mu\text{m}$  which is amplified by the hydraulic converter to 750  $\mu\text{m}$  at the actuator head at a frequency of 200 Hz.

(further acquisition parameters: FoV = 60 mm; MEG cycles = 2-4 ; MEG amplitude = 95 mT/m; flip angle = 30 ; TR = 135 ms; TE = 16.2 ms). Fourier-transforming and scaling of  $\phi(x,y,t)$  yielded the complex shear wave image  $U(x,y,f)$ .  $G^*(x,y,f)$  was calculated from  $U(x,y,f)$  by a 2D-inversion of the Helmholtz equation and spatially averaged over a wave energy-adapted region of interest.

**Results:** Examples of waves of different frequency inside a rat liver are displayed in figure 2. There were no driver-related image artifacts impairing the processing of MRE wave data. The data displayed an excellent illumination of the rat liver by shear waves. Figure 2 shows that wavelengths and wave amplitudes decrease with drive frequency. Real part ( $G'$ ) and imaginary part ( $G''$ ) of  $G^*$ , also referred to as storage and loss modulus, are shown in figure 3. The strong frequency dispersion observed for  $G'$  indicates pronounced viscous properties of rat liver.

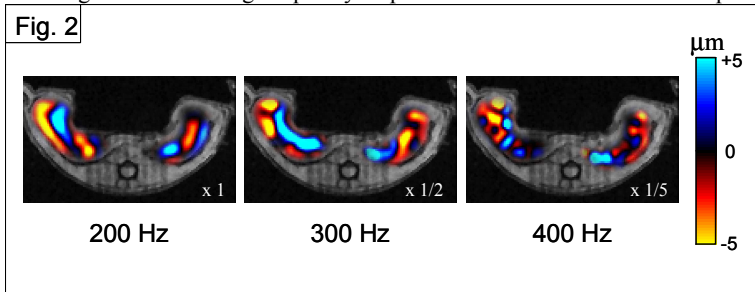


**Figure 2:** MRE examinations on in vivo rat liver. Complex wave images (real part) are illustrated for all applied mechanical excitation frequencies. Deflection values for the 300 Hz and 400 Hz vibrations have to be scaled by the factors given in the images.

**Discussion and Conclusion:** This study presents initial results with hydraulic transmission of vibrations inside an MRI scanner. This is a novel concept of motion generation in MRE. The passive driver connected to the pneumatic tube can be flexibly adjusted to different positions and organs of the animal. Neither magnetic field interactions nor interferences with the imaging system were produced. Excellent wave penetration of rat liver in the desired frequency range could be achieved. The deduced shear modulus data are reproducible and consistent with literature values [5]. Our results stimulate further effort to use the new driver system as standard motion generator in MRE on small animals and to transfer this concept to humans.

**References:** [1] Muthupillai et al., Science 269, 1854-1857 (1995) ; [2] Salameh et al., Radiology 253, 90-7 (2009); [3] Talwalkar et al., Hepatology 47 (1), 332-342 (2008) ; [4] Uffmann et al., IEEE Engin Med Biol May/June, 28-34 (2008), [5] Salameh et al., J Magn Reson Imaging 26, 956-62 (2007),

**Methods:** The proposed driver system based on a piezo-stack of 130 mm length (Physik Instrumente, Karlsruhe, Germany) and a pneumatic transmission tube is described in figure 1. A gradient echo based MRE acquisition sequence was implemented on a 4.7 T Biospec scanner (Bruker Biospin, Ettlingen, Germany). Shear waves were induced by a hydraulic actuator with excitation frequencies of 200 Hz, 300 Hz, and 400 Hz applied to a central, transversal image slice through the liver of male healthy Wistar rats (average weight 300 g). The actuator was placed directly over the liver, tightly connected with the animal bed and placed in the center of the MRI scanner. A tripilot scan was acquired for appropriate slice selection. Out-of-plane motion encoding was chosen for shear waves generated by the vertically vibrating actuator head. The frequency of the motion encoding gradient (MEG) was matched to the mechanical excitation frequency. Steady state conditions were achieved using dummy oscillations before the start of the motion encoding gradient (MEG). In all examinations 4 time-resolved phase-difference images  $\phi(x,y,t)$  with a 128x128 matrix size were acquired

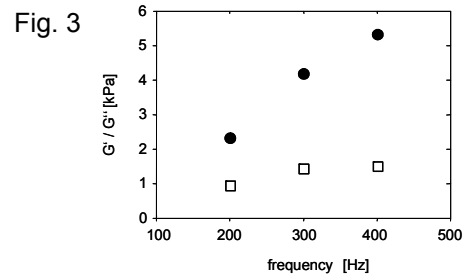


**Figure 3:** Storage modulus  $G'$  (full symbols) and loss modulus  $G''$  (open symbols) for the measured data.